SiF 2022– The 12th International Conference on Structures in Fire
The Hong Kong Polytechnic University, Nov 30 - Dec 2, 2022

COMPARATIVE ANALYSIS OF THE FIRE PERFORMANCE OF A STEEL ARCH BRIDGE

Patrick Covi[1], Nicola Tondini[2], Enrico Giuriati[3]

ABSTRACT

Bridges are strategic infrastructures and must be designed to withstand operating and exceptional load conditions. However, the current structural standards of bridges do not explicitly consider fire actions. In fact, unlike most structures and infrastructures (buildings and tunnels), there is no specific regulatory obligation that requires the designer to verify a bridge according to fire resistance criteria. However, the fire risk is not negligible, as highlighted by the scientific literature. This aspect can lead to a high vulnerability to the fire of bridges and in the event of a fire, a significant impact on the functionality of the infrastructural network can therefore be expected. The present work fits into this context by analyzing the fire vulnerability of an arched steel overpass with an orthotropic slab deck. Different plausible fire scenarios, such as heavy good trucks, were considered below the bridge and were modelled according to nominal curves and natural fire curves, such as computational fluid dynamics (CFD). A series of thermomechanical analyses were then developed to identify the failure modes and times of collapse, as well as the deformation behaviour that can cause the loss of functionality.

Keywords: Arch bridge, fire, CFD, orthotropic deck.

1 INTRODUCTION

The safety of road networks is a fundamental prerequisite for the economy, the environment, and society. The most vulnerable elements in a road network are bridges. Several researchers have studied bridge failures and monitoring systems [1-6]. The causes of collapses include flood, earthquake, fire, collision, wind, overload, settlement, and environmental degradation of the bridge elements.

Fire is an action that can severely damage bridge structures, which are not generally designed with fire resistance criteria. In addition, to assess the possibility of structural collapse, which can occur despite the beneficial effect of the ventilation that cools the hot gas that spreads during the fire, it is often essential to check the extent of the deformations in the structure. In fact, too high deformations not only may cause the loss of functionality of the bridge, with severe repercussions for vehicular traffic, but can also cause damage to systems and underground services, both urban and extra-urban, often incorporated into the structure, with even more extensive consequences.

[1] Postdoctoral Researcher, Department of Civil, Environmental and Mechanical Engineering, University of Trento (Italy)
e-mail: patrick.covi@unitn.it, ORCID: https://orcid.org/0000-0002-0570-4061
[2] Associate Professor, Department of Civil, Environmental and Mechanical Engineering, University of Trento (Italy)
e-mail: nicola.tondini@unitn.it, ORCID: https://orcid.org/0000-0003-2602-6121
[3] MSc student, Department of Civil, Environmental and Mechanical Engineering, University of Trento (Italy)
e-mail: giuriati.enrico@gmail.com

In recent years, several researchers have studied the structural behaviour of bridges subject to fire scenarios using numerical models [7-16], experimental tests [17-18], fire behaviour bridge girders [8,20], and more generally on the fire risk applied to bridges [22-26].

Among these, the research by Moya et al. (2014) [9] concerned the study of the fire that occurred at the I-65 flyover in Birmingham, Alabama, USA in 2002 through numerical analysis. Some computational fluid dynamics models (CFD) were used to reproduce the real fire scenario during the accident.

The research conducted by Dotreppe et al. (2006) [15] concerned the Vivegnis bridge near Liège, a Tied-arch bridge made of steel and a composite steel-concrete deck. The bridge collapsed following a fire caused by a gas pipe explosion. Several numerical simulations were performed with the SAFIR software to simulate the behaviour of the bridge subject to a localized fire. Choi (2008) [16] conducted numerical analyses of the behaviour of the I-80/880 junction bridge in Oakland (USA) during the fire that destroyed part of the composite steel-concrete deck. Some experimental campaigns were also carried out on bridges subject to the action of fire, including the experimental tests conducted by Moya et al. (2017) [18] concerned a bridge with steel beams and reinforced concrete slab. A six meter span bridge subjected to four realistic fire scenarios.

Zhang et al. [20] presented an overview on fire behaviour of bridge girders. Bridge girders subject to fire could exhibit a large deflection or, in some cases, torsion and lateral-torsion problems [20]. Possidente et al. [21] developed a 3D-beam finite element code to model open cross-section steel elements subjected to torsional and lateral-torsion effects under fire condition.

Garlock et al. (2012) [24] presented a detailed overview of bridges that have been subject to fires in the past, post-fire repair strategies in bridges and an overview of the fire risk in bridges. Kodur et al. (2021) [29] examined the risk of fires in transport infrastructure such as bridges and tunnels. In particular, some strategies were analysed to mitigate the fire risks in these types of structures. Finally, the research by Khan et al. (2021) [26] developed a framework for assessing the fire risk of bridges based on data from six case studies.

In 2002, average annual losses of $1.28 billion from fire-damaged bridges were estimated in the United States alone. In particular, the fires that are triggered on the infrastructural network are mainly caused by the collision of vehicles with combustible materials and gas explosion from a leaking pipeline attached to the bridge structure [29-30]. Therefore, their intensity can be exceptionally high, also due to the fact that collisions produce the rapid ignitions of highly flammable materials. Bridges and overpasses with girders and with cables / stays made of steel and steel-concrete composite are therefore particularly vulnerable, since: i) being in most cases not designed with fire resistance criteria, the load-bearing capacity decreases rapidly due to the rapid heating of the steel structural elements and ii) are often made with statically determined schemes with low robustness in case of fire. Furthermore, the closure of a bridge can have significant repercussions on the infrastructural network and economic consequences.

2 CASE STUDY

(a) (b)

Figure 1. General view of the bridge (3D render): (a) Highway overpass; (b) Overpass on a suburban area.

The bridge geometry, material models and other assumptions are provided in this section. The bridge analyzed in this paper is an unprotected single-span steel arch overpass, as shown in Figure 1. The bridge is 65 m long and 14.7 m wide and it consists of an orthotropic slab deck with two traffic lanes. The transverse beams are placed every 3 m. Figure 2 shows its cross section and some tridimensional render details. The bridge has one arch along the span that is centred in the middle of the bridge deck. The steel bridge deck is fully fixed at the junction of the arch and provides lateral stability to the arch. Two different steel grades were used. In detail, high-strength steel grade (fy ≥ 750 N/mm^2) was adopted for the hangers, while steel grade S355 (EN 10025-2, 2019) was adopted for all other elements, i.e. steel deck and arch.

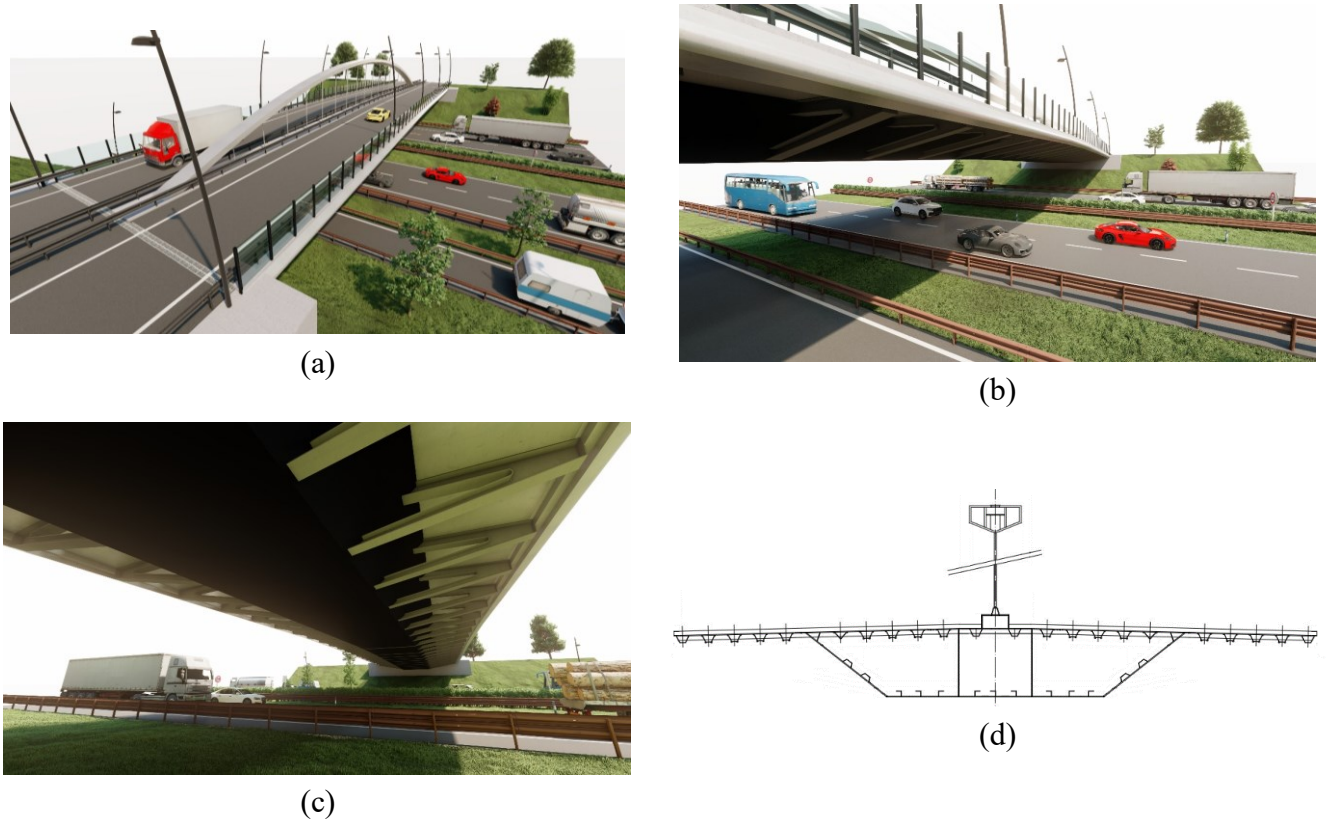

Figure 2. (a-c) 3D render details; (d) Section of the bridge.

3 FEM

Typically, the restraints at the end of the bridge are considered as free or fixed end conditions (Figure 3a-b). Bridges and the infrastructures anchored to them (i.e. pipes, electrical cables, monitoring systems) are designed to allow thermal expansion within certain displacement limits using thermal joints [31-33]. Maximum and minimum air temperature values are used to estimate the axial displacements of the bridge due to thermal expansion and expansion joints are designed to accommodate them. However, when a fire occurs, the thermal expansions can be higher than the maximum displacement of the designed expansion joint. In this scenario, the presence of the thermal joints induces restraint conditions that are in between the two limit cases (Figure 3c).

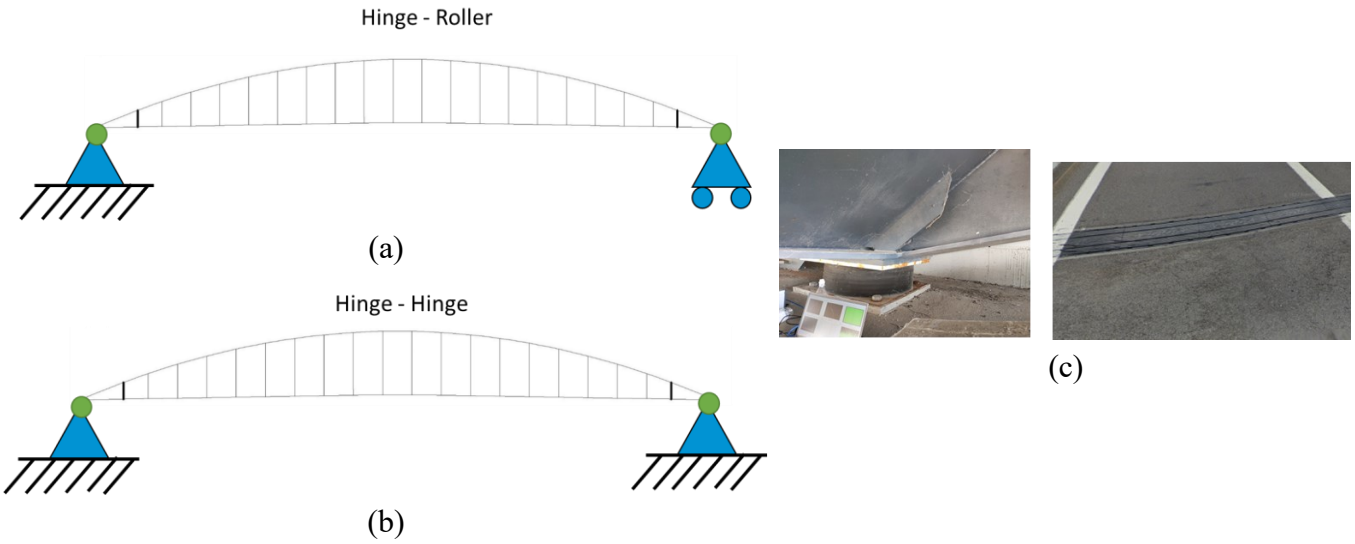

Figure 3. (a) bridge free end condition; (b) bridge fixed end condition; (c) dissipator and thermal joint.

In this respect, SAFIR [34] does not include a gap element to model expansion joints. Since it is a proprietary software, it was not possible to implement a GAP element directly in the source code. Therefore, a different approach was used in order to implement the GAP with only the elements already inside the SAFIR software. Figure 4 illustrates the configuration of the mechanical system that was used to simulate the GAP.

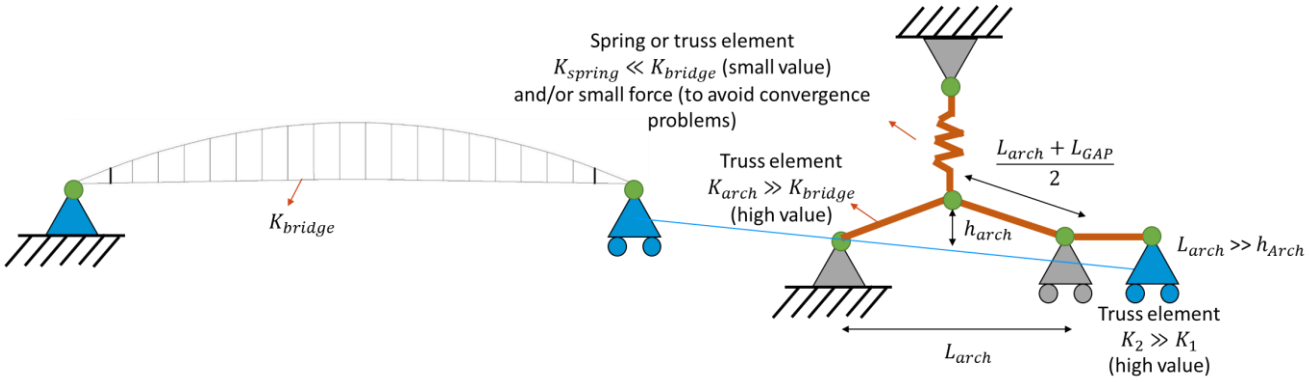

Figure 4. mechanical configuration to simulate the bridge's gap.

The mechanical system works in a similarly to a Von Mises Planar Truss/Arch [35] and a Pantograph. The system was made of two straight hinges truss elements for the arch and a third horizontal truss element that connects the arch with the rest of the structure. To avoid convergence problems due to the lability condition or snap-through and to have a small force in order to re-open the GAP, a spring was applied at the crown of the arch.

The system can extend along the horizontal axis for the desired displacement of the bridge thermal joint (L_{GAP}). Based on the geometrical parameter of the mechanism, such as the desired gap length (L_{GAP}) and the initial span of the arch (L_{arch}), it is possible to obtain the initial height of the arch (h_{arch}) using Equation 1.

$$h_{arch} = \sqrt{\frac{L_{GAP}}{2} * \left(L_{arch} + \frac{L_{GAP}}{2}\right)} \qquad (1)$$

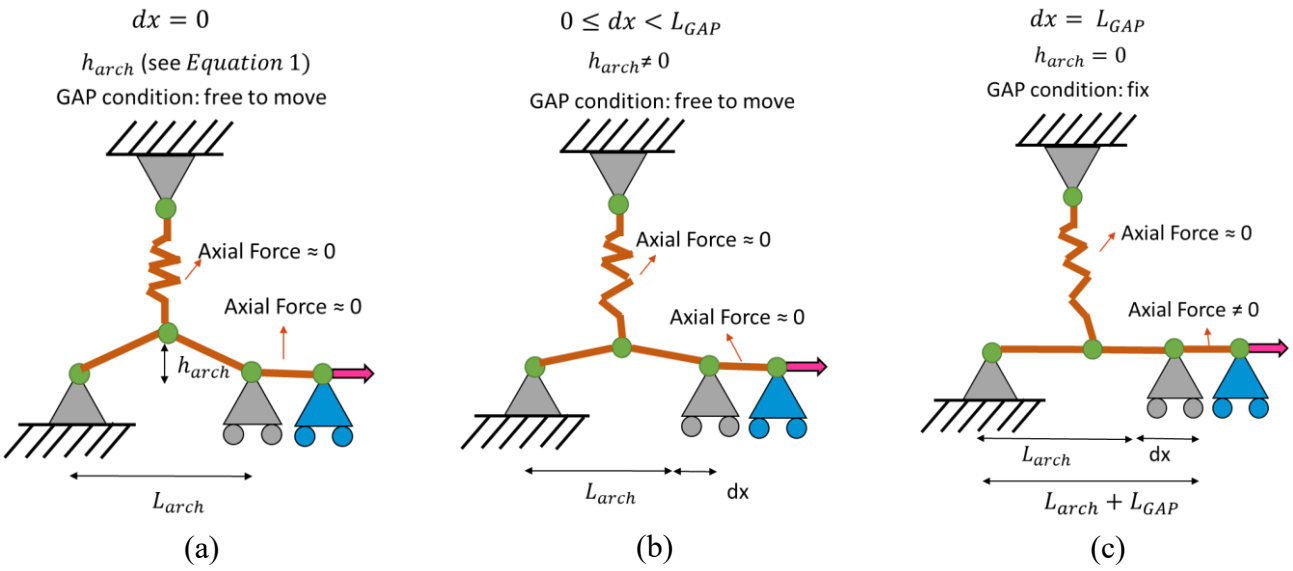

Figure 5. Operation of the mechanical system (GAP): (a) at rest; (b) partially opened; (c) fully closed.

Figure 5 illustrates the mechanism during different steps. In detail, Figure 5a shows the GAP mechanism at rest. When the bridge or the structures starts to expand, the arch starts closing, giving a minimal resistance to the horizontal movement of the structure that could be considered negligible (see Figure 5b). Finally, when the maximum length of the GAP setting is reached, the GAP is fully closed and prevents the bridge or the structure from moving forward in the horizontal direction, as shown in Figure 5c.

The spring force should not be too big or small value to avoid convergency problems caused by out-of-range values in the matrix operations. For the same reason, the stiffness of the truss elements must not be a very high value. A round cross-section with area equal to A = 1.0 m^2, Young's modulus E = 6000 GPa was chosen for the truss elements.

In order to demonstrate the effectiveness of the GAP methodology and to illustrate the implementation of a real scenario using SAFIR, the proposed mechanical system was added to a simply supported beam. Results of the SAFIR analysis were then verified against the GAP element developed in the software OpenSees [36]. Figure 6a shows the numerical model of the simply supported beam with the GAP mechanism in both horizontal directions, while Figure 6b illustrates the horizontal input force imposed at the end of the beam. Figure 6c compares the horizontal displacement responses measured at the end of the beam; instead, Figure 6 compares the force of the GAP element. As can be appreciated in Figure 6c-d, the structure's response obtained using SAFIR well matches the reference OpenSees solution.

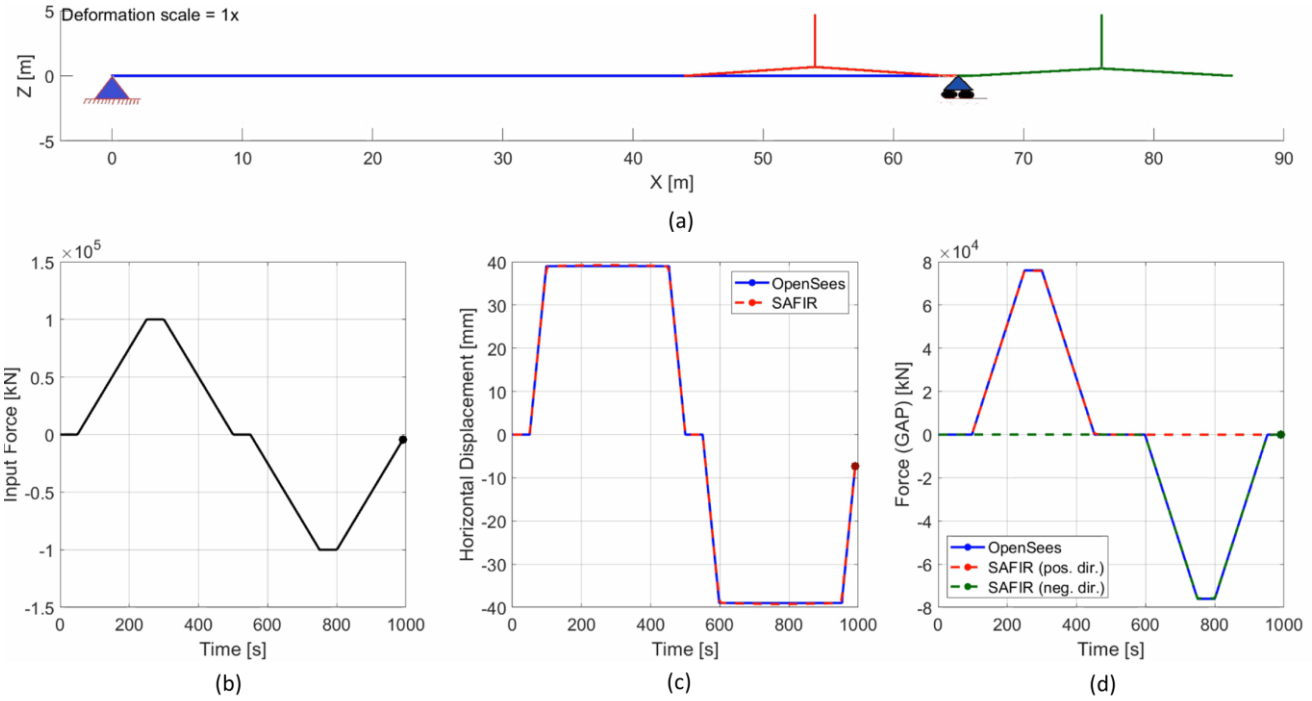

Figure 6. Comparison between SAFIR and OpenSees: (a) FEM model with the GAP mechanism in both horizontal directions. (b) Horizontal input force; (c) horizontal displacement; (d) Axial forces of the GAP mechanism.

A 3D thermomechanical model of the bridge was created in the thermomechanical software SAFIR using nonlinear Euler-Bernoulli beam elements, as shown in Figure 7.

In this work, modelling the gap that simulates the thermal expansion joints of the bridge was considered. In detail, a gap of 0.2 m was modelled to allow for the thermal expansion of the bridge up to the end of the thermal joint. A series of thermomechanical analyses were performed to investigate the structural fire behaviour, including the deformation behaviour that can cause the loss of functionality of the bridge.

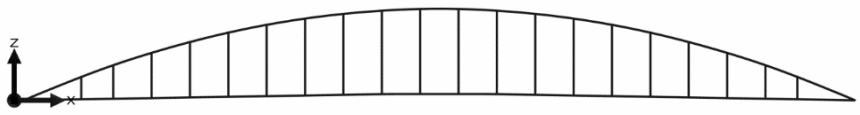

Figure 7. Numerical model

4 FIRE ANALYSIS

Both a prescriptive and a performance-based approach were applied by employing different fire curves and by selecting different plausible fire scenarios. Indeed, the most common way to define the gas temperature is to use prescriptive code-based fire curves. Therefore, preliminary analyses were performed using nominal curves such as the hydrocarbon and the ISO 834 curve, the former being more appropriate, as illustrated in Figure **9**. Another type of curve used to analyse the fire behaviour of bridges is the fire curve proposed by Stoddard [37] (see Fig. 4). This curve was conceived to estimate the air temperature following a collision between tanker trains, which happened on 11 December 2002.

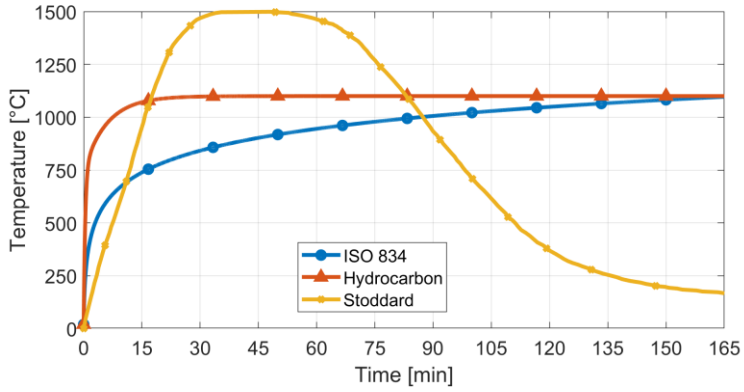

Figure 8. prescriptive code-based fires curves and Stoddard curve

Because of the length of the bridge, a vehicle fire will naturally induce a non-uniform thermal action on the structure. Indeed, the nominal fire curves were applied not only to the whole length of the bridge but to different portions, i.e. total length, half-length and one quarter, as illustrated in Figure 9.

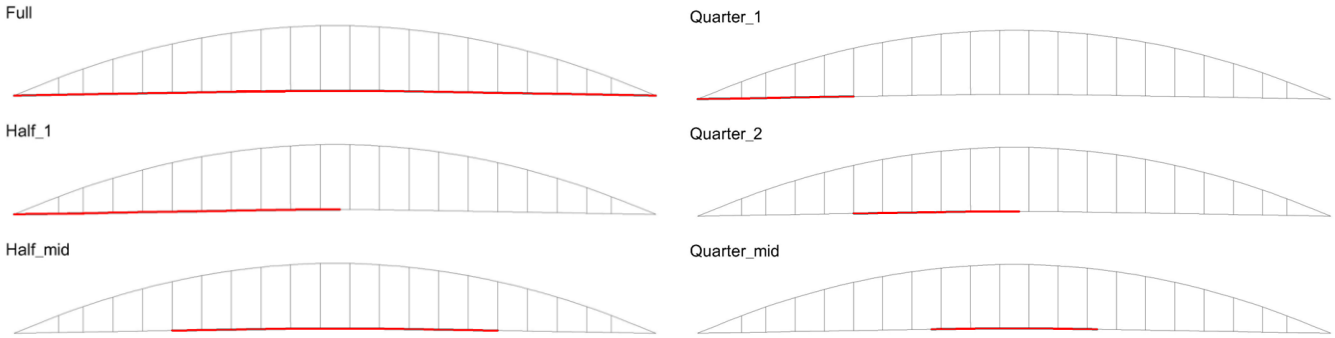

Figure 9. Portion of the bridge under fire action

The simulation results using the nominal fire curves are summarized in Table 1. It is possible to observe that applying the fire curve to the entire bridge length leads to structural failure. The Stoddard fire curve was the more severe and entailed the collapse under all heating configurations. No structural failure was observed when the bridge was half heated for the ISO 834 and the hydrocarbon fire curve. In terms of residual deformation, all maximum vertical displacement values exceed L/150. By assuming a limit value of L/250 as for the serviceability limit state for steel structures, the full functionality of the bridge cannot be assured.

Table 1. Results of the prescriptive code-based fires curves and Stoddard curve.

ID	Nominal curve	Fire location	(min)	Residual deflection (m)	Residual deflection over bridge's length
#1	ISO834	Full	64	Not applicable	Collapse
#2	ISO834	Half_1	102	-0.49	L/135
#3	ISO834	Half_Mid	120	-0.45	L/145
#4	ISO834	Quarter_1	120	-0.48	L/135

#5	ISO834	Quarter_2	120	-0.46	L/140
#6	ISO834	Quarter_Mid	120	-0.46	L/140
#7	Hydrocarbon	Full	28	Not applicable	Collapse
#8	Hydrocarbon	Half_1	55	-0.47	L/140
#9	Hydrocarbon	Half_Mid	78	-0.51	L/130
#10	Hydrocarbon	Quarter_1	120	-0.48	L/135
#11	Hydrocarbon	Quarter_2	120	-0.46	L/140
#12	Hydrocarbon	Quarter_Mid	120	-0.46	L/140
#13	Stoddard	Full	28	Not applicable	Collapse
#14	Stoddard	Half_1	38	Not applicable	Collapse
#15	Stoddard	Half_Mid	32	Not applicable	Collapse
#16	Stoddard	Quarter_1	42	Not applicable	Collapse
#17	Stoddard	Quarter_2	42	Not applicable	Collapse
#18	Stoddard	Quarter_Mid	41	Not applicable	Collapse

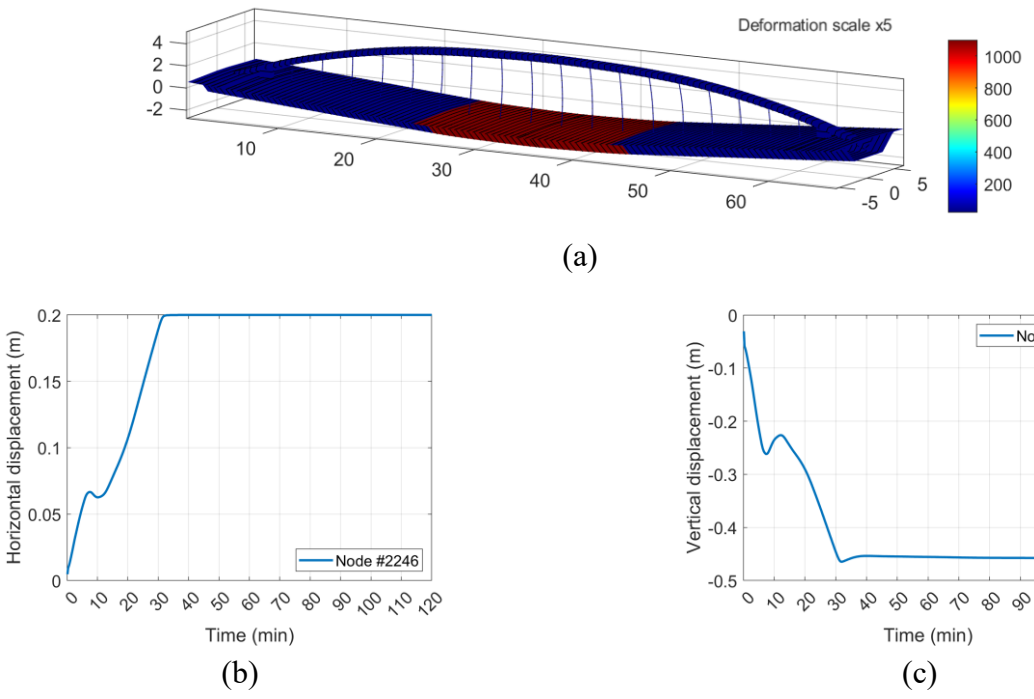

Figure 10. Analysis #12: Results at the end of the simulation: (a) Deformed shape and steel temperature; (b) Horizontal displacement; (c) Vertical displacement at mid-span.

Figure 10b-c illustrates the horizontal and vertical displacement responses measured respectively at the end node and mid-span node of the bridge. It is worth pointing out that a 0.2 m expansion joint effect was included and after 38 minutes the axial expansion of the bridge reaches the gap, as shown in Figure 10b. It is possible to notice an inversion of the horizontal and vertical displacements between 7 minutes and 13

minutes from the beginning of the fire. This is caused by the vertical variation of the stiffness center caused by the differential increase in the temperatures in the section.

Moreover, different plausible natural fire scenarios were also considered, such as heavy good trucks, below the bridge and they were modelled according to computational fluid dynamics (CFD) models using FDS (Fire Dynamics Simulator) software [38]. A 3D model of the bridge has been created. The model domain was 65.0 m wide, 20.0 m deep and 15.0 m high to allow the fire sufficient volume for air entrainment and extension of flames. All boundaries were left open to ambient and the initial temperature was 20°C. The model included the ground slope. The geometry of the modelled bridge is shown in Figure 11.

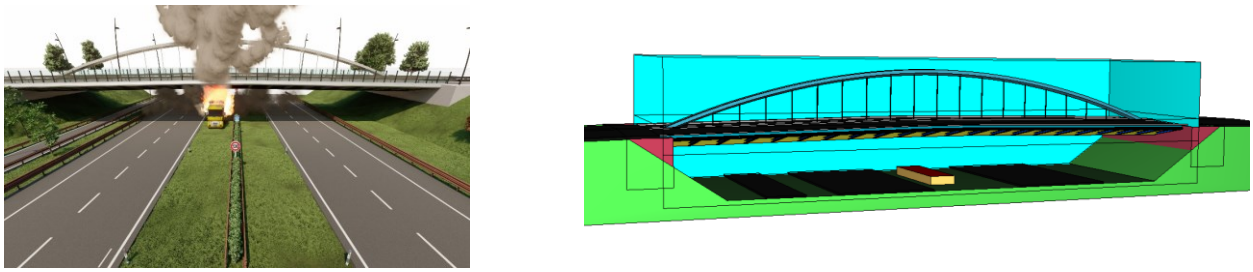

(a) (b)

Figure 11. FDS fire scenario (Truck location A) a) 3d render b) FDS general view.

In order to model a real fire in a CFD analysis, it is possible to apply an HRR (Heat Release Rate) thermal release curve, as also described in the Italian Ministerial Fire Prevention Decree of 3 August 2015 (DM 3AGO (2015)) (Fire Prevention Code). The HRR curve is the variation of the thermal release power in a combustion reaction, which depends on the fuel, the ventilation conditions and the geometric characteristics of the material.

One HRR curve was used for the simulations:

- Truck: the heavy goods vehicle loaded with wood and plastic pallets (Figure 12) [39].

The fires were placed in four different locations underneath the bridge:

- Location A: the fire was centered at mid-span, both longitudinally and transversely (Figure 13).
- Location B: The fire location was offset longitudinally from the center of the bridge near the end of the bridge.

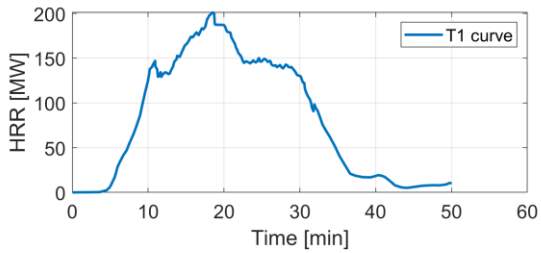

Figure 12. HRR of the heavy goods vehicle loaded with wood and plastic pallets [39].

Figure 13 illustrates the development of fire and smoke after 23 minutes from the beginning of one fire scenario as an example of the fire development stages.

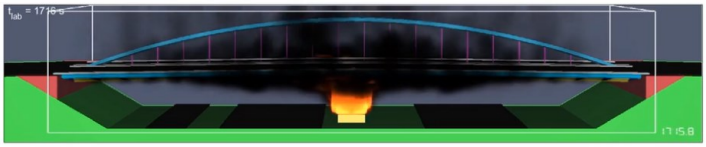

Figure 13. FDS results general view of the bridge after 25 min (Truck location A).

To measure the temperature evolution of the gas, a total of 2022 adiabatic surface temperature gas-phase devices were placed across the bridge deck, arch and hangers. The output values from these devices were used for performing thermal-structural analysis of the sections in SAFIR.

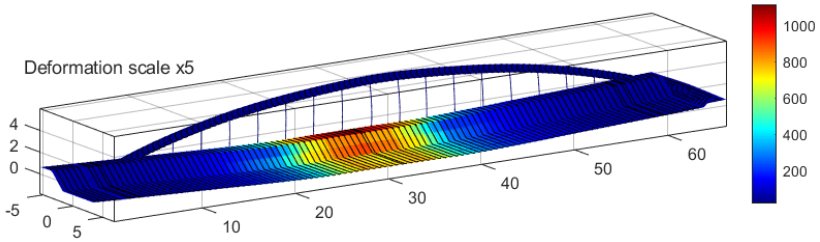

Figure 14. Deformed shape and steel temperature of the deck after 25 min.

The simulation results using the FDS scenarios are summarized in Table 2. As an example, Figure 14 shows the deformed configuration and steel temperature of the deck 23 minutes after the beginning of the fire scenario modelled in FDS that involved the heavy goods vehicle loaded with wood and plastic pallets. Figure 15 illustrates the horizontal and the deflection time history of the bridge under the FDS fire load. No structural failure was observed with residual vertical displacement between 20 cm (L/310) and 30 cm (L/240) depending on the fire scenario. In this case, given the fact that a smaller part of the bridge is affected by the fire, it is not trivial to state that a residual displacement less than L/250 can lead to full functionality because the deformation can be highly localised with steep gradients of vertical displacement near the maximum value. This should be investigated more in depth.

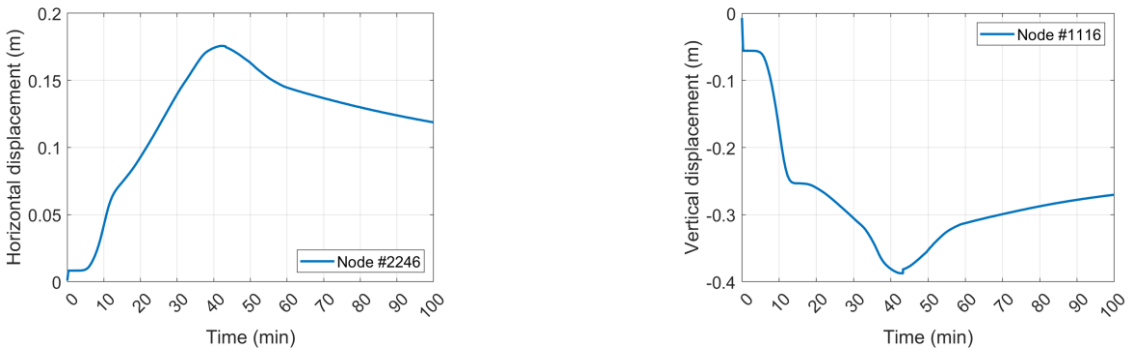

Figure 15. Displacements time history of the bridge: (a) Horizontal; (b) Deflection.

Table 2. Results of the FDS scenarios.

ID	Nominal curve	Fire location	(min)	Residual deflection (m)	Residual deflection over bridge's length
#1	Truck	Location A	100	-0.27	L/240
#2	Truck	Location B	100	-0.21	L/310

5 CONCLUSIONS

The paper presented numerical fire analysis and thermal-structural analysis to investigate a steel arch bridge under fire using CFD and SAFIR software.

The results showed that nominal curves are generally conservative and predict much shorter failure times. CFD analyses provided more realistic representations of the bridge fire scenario and in the analysed cases the collapse was not even attained. However, in all cases in which failure was not reached, the final deformation state was to such an extent that the bridge was not fully functional after fire for nominal fire curves by assuming a vertical limit of L/250. For the CFD analyses, smaller residual deformations were observed, but more localised. The modelling of the expansion joint (GAP) in the numerical model allowed to obtain a more realistic constraint condition compared to the boundary conditions frequently used in other studies, such as hinge-hinge or hinge-roller constraints.

ACKNOWLEDGMENT

The support received from the Italian Ministry of Education, University and Research (MIUR) in the framework of the 'Departments of Excellence' (grant L 232/2016) is gratefully acknowledged

REFERENCES

1. Lee, G. C., Mohan, S., Huang, C., & Fard, B. N. (2013). A study of US bridge failures (1980-2012). Buffalo, NY: MCEER.
2. Scheer, J. (2011). Failed bridges: case studies, causes and consequences. John Wiley & Sons.
3. Diaz, E.E.M., Moreno, F.N., and Mohammadi, J. (2009). Investigation of Common Causes of Bridge Collapse in Colombia. Practice Periodical on Structural Design and Construction. 14(4): p. 194-200
4. Deng L, Wang W, Yu Y (2016) State-of-the-art review on the causes and mechanisms of bridge collapse. J Perform Constr Facil. https://doi.org/10.1061/(ASCE)CF.1943-5509.0000731
5. Ceravolo R., Tondini N.*, Abbiati G. and Kumar A. (2012) Dynamic characterization of complex bridge structures with passive control systems. Structural Control and Health Monitoring, 19(4): 511–534. doi: 10.1002/stc.450.
6. Tonelli, D., Rossi, F., Brighenti, F. et al. Prestressed concrete bridge tested to failure: the Alveo Vecchio viaduct case study. J Civil Struct Health Monit (2022). https://doi.org/10.1007/s13349-022-00633-w
7. Payá-Zaforteza, I. and Garlock, M.E.M., 2012. A numerical investigation on the fire response of a steel girder bridge. Journal of Constructional Steel Research, 75, pp.93-103.
8. Aziz, E. and Kodur, V., 2013. An approach for evaluating the residual strength of fire exposed bridge girders. Journal of Constructional Steel Research, 88, pp.34-42.
9. Alos-Moya, J., Paya-Zaforteza, I., Garlock, M. E. M., Loma-Ossorio, E., Schiffner, D., & Hospitaler, A. (2014). Analysis of a bridge failure due to fire using computational fluid dynamics and finite element models. Engineering Structures, 68, 96-110.
10. Liu, Z., Silva, J.C.G., Huang, Q., Hasemi, Y., Huang, Y. and Guo, Z., 2021. Coupled CFD–FEM Simulation Methodology for Fire-Exposed Bridges. Journal of Bridge Engineering, 26(10), p.04021074.
11. Song, C., Zhang, G., Kodur, V., Zhang, Y. and He, S., 2021. Fire response of horizontally curved continuous composite bridge girders. Journal of Constructional Steel Research, 182, p.106671.
12. Timilsina, S., Yazdani, N. and Beneberu, E., 2021. Post-fire analysis and numerical modeling of a fire-damaged concrete bridge. Engineering Structures, 244, p.112764.
13. Alos-Moya, J., Paya-Zaforteza, I., Hospitaler, A. and Loma-Ossorio, E., 2019. Valencia bridge fire tests: Validation of simplified and advanced numerical approaches to model bridge fire scenarios. Advances in Engineering Software, 128, pp.55-68.
14. Zhang, G., Song, C., Li, X., He, S. and Huang, Q., 2021. Fire performance of continuous steel-concrete composite bridge girders. KSCE Journal of Civil Engineering, 25(3), pp.973-984.
15. Dotreppe JC, Majkut S, Franssen JM. 2006. Failure of a tied-arch bridge submitted to a severe localized fire, structures and extreme events. IABSE Symposium; p. 272–273.
16. Choi J. (2008) Concurrent fire dynamics models and thermomechanical analysis of steel and concrete structures. Ph.D. dissertation. Atlanta (USA): Georgia Institute of Technology.
17. Kaundinya, I., Bergerhausen, U. and Schmidt, J., 2017. Effects of extreme fire scenarios on bridges. Bridge Structures, 13(4), pp.159-167.

18. Alos-Moya, J., Paya-Zaforteza, I., Hospitaler, A. and Rinaudo, P., 2017. Valencia bridge fire tests: Experimental study of a composite bridge under fire. Journal of Constructional Steel Research, 138, pp.538-554.
19. Thiébaud, R., Lebet, J. P., Beyer, A., & Boissonnade, N. (2016). Lateral torsional buckling of steel bridge girders. In Proceedings of the Annual Stability Conference Structural Stability Research Council, Orlando, USA (pp. 12-15).
20. Zhang, G., Zhao, X., Lu, Z., Song, C., Li, X., & Tang, C. (2022). Review and discussion on fire behavior of bridge girders. Journal of Traffic and Transportation Engineering.
21. Possidente L., Tondini N.*, Battini J.-M. (2020) 3D beam element for the analysis of torsional problems of steel structures in fire, Journal of Structural Engineering, 146:(7), 10.1061/(ASCE)ST.1943- 541X.0002665.
22. Naser, M.Z. and Kodur, V.K.R., 2015. A probabilistic assessment for classification of bridges against fire hazard. Fire Safety Journal, 76, pp.65-73.
23. Aziz, E.M., Kodur, V.K., Glassman, J.D. and Garlock, M.E.M., 2015. Behavior of steel bridge girders under fire conditions. Journal of Constructional Steel Research, 106, pp.11-22.
24. Garlock, Maria, et al. "Fire hazard in bridges: Review, assessment and repair strategies." Engineering structures 35 (2012): 89-98.
25. Kodur, Venkatesh, and M. Z. Naser. "Fire hazard in transportation infrastructure: Review, assessment, and mitigation strategies." Frontiers of Structural and Civil Engineering (2021): 1-15.
26. Khan, M.A., Khan, A.A., Anwar, G.A. and Usmani, A., 2021, October. Framework for fire risk assessment of bridges. In Structures (Vol. 33, pp. 523-532). Elsevier.
27. Possidente L., Tondini N.*, Battini J.-M. (2020) 3D beam element for the analysis of torsional problems of steel structures in fire, Journal of Structural Engineering, 146:(7), 10.1061/(ASCE)ST.1943- 541X.0002665.
28. Aziz, E.M., Kodur, V.K., Glassman, J.D. and Garlock, M.E.M., 2015. Behavior of steel bridge girders under fire conditions. Journal of Constructional Steel Research, 106, pp.11-22.
29. Kodur, Venkatesh, and M. Z. Naser (2021) "Fire hazard in transportation infrastructure: Review, assessment, and mitigation strategies." Frontiers of Structural and Civil Engineering.
30. Hu, Jiayu, Ricky Carvel, and Asif Usmani. (2021) "Bridge fires in the 21st century: A literature review." Fire Safety Journal.
31. Roeder, C. W. (2003). Proposed design method for thermal bridge movements. Journal of Bridge Engineering, 8(1), 12-19.
32. Parke, G., & Hewson, N. (Eds.). (2022). ICE manual of bridge engineering. ICE Publishing.
33. Caspani, V.F.; Tonelli, D.; Poli, F.; Zonta, D. Designing a Structural Health Monitoring System Accounting for Temperature Compensation. Infrastructures 2022, 7, 5. https://doi.org/10.3390/infrastructures7010005
34. Franssen, J-M, Gernay, T. (2017): Modeling structures in fire with SAFIR©: Theoretical background and capabilities. Journal of Structural Fire Engineering, 8 (3), 300-323.
35. R. von Mises, “Über die Stabilitätsprobleme der Elastizitätstheorie,” ZAMM, vol. 3, pp. 406–422, 1923
36. McKenna, F. (2011). “Opensees: a framework for earthquake engineering simulation,”Computing in Science & Engineering, vol. 13, no. 4,pp. 58–66.
37. Stoddard R. (2004), “Inspection and repair of a fire damaged prestressed girder bridge,” in Proceedings of International Bridge Conference, Pittsburgh, PA, USA.
38. McGrattan, K. , McDermott, R. , Weinschenk, C. and Forney, G. (2013), Fire Dynamics Simulator, Technical Reference Guide, Sixth Edition, Special Publication (NIST SP), National Institute of Standards and Technology, Gaithersburg, MD, [online], https://doi.org/10.6028/NIST.sp.1018
39. Hurley, M. J., Gottuk, D. T., Hall Jr, J. R., Harada, K., Kuligowski, E. D., Puchovsky, M., and Wieczorek, C. J. (Eds.). (2015). SFPE handbook of fire protection engineering. Springer.